

Article

# Photoluminescence of Rare-Earth Ions in the Nanocrystalline GaAs/SnO<sub>2</sub> Heterostructure and the Photoinduced Electrical Properties Related to the Interface

Diego H. O. Machado, Luis V. A. Scalvi \* and Cristina F. Bueno

Department of Physics – FC, UNESP- São Paulo State University, 17033-360 Bauru, Brazil; diegomachado@fc.unesp.br (D.H.O.M.); cris@fc.unesp.br (C.F.B.)

\* Correspondence: scalvi@fc.unesp.br; Tel.: +55-14-3103-6084

Academic Editors: Augusto Marcelli and Antonio Bianconi

Received: 31 October 2016; Accepted: 24 January 2017; Published: 7 February 2017

**Abstract:** Deposition of an SnO<sub>2</sub> thin film was carried out by sol–gel-dip-coating and doped with Ce<sup>3+</sup> or Eu<sup>3+</sup>, and a GaAs layer was deposited by resistive evaporation or sputtering. This investigation combines the emission properties of these rare-earth ions with the unique transport properties generated by the heterostructure assembly. Illumination with light with energy above the GaAs bandgap and below the SnO<sub>2</sub> bandgap drastically increases the GaAs/SnO<sub>2</sub> heterostructure conductance, which becomes practically temperature-independent. This was associated with the presence of interface conduction, possibly a two-dimensional electron gas at the GaAs/SnO<sub>2</sub> interface. This feature takes place only for the sample where the GaAs bottom layer is deposited via sputtering. Irradiation with energies above the SnO<sub>2</sub> bandgap only excites the top oxide layer. The heterostructure assembly GaAs/SnO<sub>2</sub>:Eu leads to emission from Eu<sup>3+</sup>, unlike SnO<sub>2</sub> deposition directly on a glass substrate, where the Eu<sup>3+</sup> transitions are absent. Eu emission comes along a broad band, located at a higher energy compared to Eu<sup>3+</sup> transitions, which are blue-shifted as the thermal annealing temperature increases. Luminescence from Ce<sup>3+</sup> ions in the heterostructure can be detected, but the ions overlap with emission from the matrix, and a cleaning procedure helps to identify Ce<sup>3+</sup> transitions.

**Keywords:** heterostructure; europium; cerium; photoluminescence; interface conduction

## 1. Introduction

The combination of light emission from rare-earth-doped oxide semiconductors and the transport properties of heterostructures is very promising for optoelectronic device design, because an efficient monochromatic light emission in a wide energy range (depending on the rare-earth used) and the possibility of controlling the carrier charge injection in order to modulate the emission as the device electrical conductivity, which allows for faster devices. Tin dioxide (SnO<sub>2</sub>) is a wide bandgap oxide semiconductor (an energy of about 3.6 eV) with more than 90% transparency in the visible range [1]. Doping SnO<sub>2</sub> with rare-earth ions reduces the thermal quenching effects [2], giving rise to high efficiency light emission. However, luminescence from thin films is not as efficient as from xerogels. Sol–gel-deposited thin films are composed of nanoscopic crystallites, which influence the emission spectra due to the particle size [3]. In thin films, the number of emission centers in the excitation source path is small, reducing emission efficiency. In this work, a heterostructure is composed with gallium arsenide (GaAs), which is widely used in applications where the interaction of light and electricity is required [4]. This property is related to preferential electron occupation in the high-mobility  $\Gamma$  valley of the conduction band, with the same crystal momentum of the valence band top. This allows direct

bandgap transition [5] that leads to efficient light emission and absorption from electronic transitions between the conduction and the valence bands, which is used today in high-efficiency laser diodes, photodetectors, and solar cells. The aim of this study is to evaluate the properties of these materials in the heterostructure format and to contribute to the optimization of this system for use for emission modulation in electro-luminescent devices.

Concerning the optical emission of rare-earth ions in the SnO<sub>2</sub> matrix, Eu<sup>3+</sup> presents basically two red emissions: <sup>5</sup>D<sub>0</sub>→<sup>7</sup>F<sub>1</sub> (around 590 nm) and <sup>5</sup>D<sub>0</sub>→<sup>7</sup>F<sub>2</sub> (around 611 nm). The first one is a magnetic dipole transition and its intensity is not affected by structural changes of the nearest neighborhood, whereas the transition <sup>5</sup>D<sub>0</sub>→<sup>7</sup>F<sub>2</sub> is ruled by electric dipoles, being hypersensitive to the local crystalline field [6]. The ratio between the areas of these emission lines, i.e.,  $A(^5D_0 \rightarrow ^7F_2) / A(^5D_0 \rightarrow ^7F_1)$  is called asymmetric ratio and tends to zero when the excited ion is located at a symmetry site, such Eu<sup>3+</sup> is substitutional to Sn<sup>4+</sup> in the SnO<sub>2</sub> lattice. On the other hand, when the sample is strongly doped, there is an increase of the asymmetric ratio, and the transition <sup>5</sup>D<sub>0</sub>→<sup>7</sup>F<sub>2</sub> becomes more evident. In addition, the shape of the photoluminescence (PL) spectra is broadened. In this case, ions are preferentially located at the grain boundary and are affected by the segregation process during growth due to excessive doping [7].

The Ce<sup>3+</sup> ion presents a 4f<sup>1</sup> electronic configuration at the ground state and 5d<sup>1</sup> at the excited state. Optical transitions between these states are electric dipole-allowed transitions. Level 5d presents strong lattice interaction, and the first dipole transition suffers a spectroscopic red shift when incorporated into a crystal, as the energy is shifted towards a lower value compared to the free ion [8]. Broad blue emission has been observed around 489 nm in a host matrix of zinc borosilicate glass [9], which is attributed to the transition from Excited Level 5d (<sup>2</sup>D) to the 4f<sup>1</sup> ground state (<sup>2</sup>F<sub>5/2</sub>) of Ce<sup>3+</sup>. Phosphors for application in LEDs have been obtained for the system Ca<sub>2</sub>SiO<sub>4</sub>:Ln (Ln = Ce<sup>3+</sup>, Eu<sup>2+</sup>, Sm<sup>3+</sup>). PL data exhibit a blue emission centered at 426 nm, attributed to Ce<sup>3+</sup> ions, from the Excited State 5d to Ground State 4f, independent of doping concentration [10]. These phosphors have potential application for LEDs close to the UV radiation range.

The radius and charge difference between the rare-earth ion and Sn<sup>4+</sup> makes ion incorporation into the SnO<sub>2</sub> lattice difficult, which leads to low quantum efficiency in the luminescence [11]. To avoid this problem, the production of materials in nanoparticle form is recommended [11], which is obtained with the sol-gel process [12].

SnO<sub>2</sub>/GaAs heterostructured thin films have been successfully obtained, giving birth to a smooth interface and improved electrical properties [13]. Photoluminescence from this sort of heterostructure, where SnO<sub>2</sub> films is doped with Eu<sup>3+</sup>, leads to the identification of rare-earth transitions, which does not happen for SnO<sub>2</sub>:Eu thin films deposited directly on top of the glass substrates, without the GaAs layer [14]. This result is reproduced here to relate the performance of the heterostructure assembly to emission properties and compare it with the Ce<sup>3+</sup>-doped device. Combinations of transparent oxides and semiconductors in the form of heterostructures have recently been presented. Promising devices for the development of solid-state lighting were achieved by *n*-ZnO/*n*-GaAs heterostructured light-emitting diodes [15]. SnO<sub>2</sub> have been successfully used with gallium selenide (GaSe) [16]. A CdTe/SnO<sub>2</sub> heterostructure has been proposed for solar cells devices [17] since the properties of CdTe can be modulated by coupling CdTe with other materials. The combination of SnO<sub>2</sub> and Al<sub>2</sub>O<sub>3</sub> layers deposited by processes similar to those of the film deposition used in this paper led to a simple device with a potential combination for use as a transparent transistor [18].

The deposition of single-crystal heterojunctions with smooth and atomic quality surfaces has become a possibility since the growth of epitaxy layers became available. If feasible, the hetero interface of GaAs and SnO<sub>2</sub> can be expected to lead to conduction and valence band offsets due to the equality in the Fermi level on both sides, originating the bending of the band diagram in the interface region [14,19]. This leads to electron confinement at the interface in a triangular shape quantum well, resulting in charge accumulation at the interface, known as two-dimensional electron gas (2DEG), with high electron mobility [13]. Although the formation of 2DEG has mostly been proposed for

semiconductor heterojunctions, 2DEG has also been found at the interface between two insulating oxides, as in the case of  $\text{LaAlO}_3$  and  $\text{SrTiO}_3$  [20].

The proposal of this work is to combine doping with trivalent rare-earth (RE)  $\text{Ce}^{3+}$  or  $\text{Eu}^{3+}$  ions in  $\text{SnO}_2$  with a GaAs layer, originating a simple heterostructure  $\text{SnO}_2:\text{RE}^{3+}/\text{GaAs}$  (or  $\text{GaAs}/\text{SnO}_2:\text{RE}^{3+}$ ). However, this kind of heterostructure, nanocrystalline in our case, is very far from any single crystal model, and it is anticipated that the interpretation and modeling of its properties will not be simple. Emission and electrical transport properties of the obtained structures are shown. PL data displays the  $\text{Ce}^{3+}$  and  $\text{Eu}^{3+}$  transitions and shows the potentiality for applications of the  $\text{SnO}_2/\text{GaAs}$  heterostructure for optoelectronic devices. For some samples, the electrical conductivity seems to be temperature-independent. In order to understand the rule of electrical transport, layers have also been grown in opposite order, i.e., with GaAs on top of  $\text{SnO}_2$ .

## 2. Results

### 2.1. Photoluminescence Results

Details on sample preparation are described in Section 4. Figure 1 shows the room-temperature luminescence spectra for two types of heterostructured samples of  $\text{GaAs}/\text{SnO}_2:2 \text{ at}\% \text{Eu}$  with distinct thermal annealing (T.A.) of the  $\text{SnO}_2$  film, as described in Section 4: at  $200^\circ\text{C}$  for 1 h (GSEu1), and at  $400^\circ\text{C}$  for 20 min (GSEu2). A PL spectra for the  $\text{SnO}_2:2\% \text{Eu}$  film thermally annealed at  $500^\circ\text{C}$  for 1 h (SEu500) is also shown. Completing the figure, PL spectra for the sample SEu1000 (films deposited on quartz and thermally annealed at  $1000^\circ\text{C}$  for 1 h) is also shown.

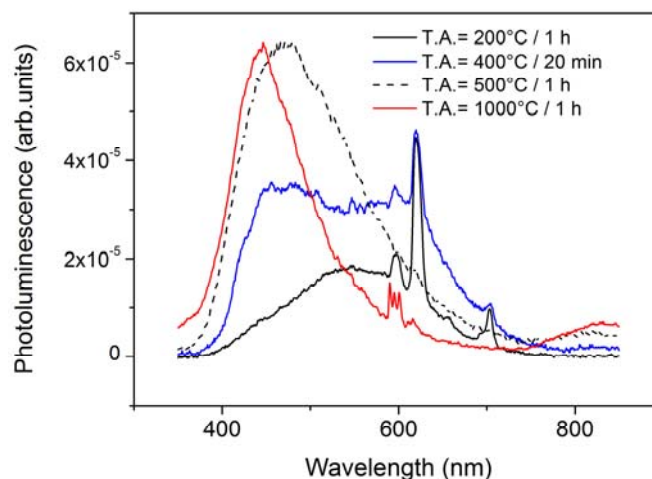


**Figure 1.** Photoluminescence for  $\text{GaAs}/\text{SnO}_2:2 \text{ at}\% \text{Eu}$  thermally annealed at  $200^\circ\text{C}$  for 1 h (sample GSEu1), and at  $400^\circ\text{C}$  for 20 min (GSEu2), as well as the  $\text{SnO}_2:2 \text{ at}\% \text{Eu}$  film treated at  $500^\circ\text{C}$  for 1 h (SEu500), and  $\text{Eu} 2\text{at}\%$ -doped  $\text{SnO}_2$  thin film deposited on a quartz substrate and thermally annealed at  $1000^\circ\text{C}$  for 1 h (SEu1000). Excitation: line 350 nm of the  $\text{Kr}^+$  laser.

Figure 2 shows the photoluminescence spectra for sample SCe1000 at 10 and 200 K, along with a deconvolution of the PL spectra measured at 10 K. In this deconvolution, four bands were obtained: two bands (blue) have maximum intensity at 410 nm, a value very close to  $\text{Ce}^{3+}$  emission, which is about 420 nm, which corresponds to the  $\text{Ce}^{3+}$  transition from Level 5d to Level 4f ( $^2F_{5/2}$ ) [21]. The other bands have peaks centered at about 457 nm and 500 nm, and are not related to  $\text{Ce}^{3+}$  transitions. Figure 2 (inset) shows the PL spectrum for the heterostructured sample GSCe2, measured at room temperature, where the signal was subtracted from the substrate signal.

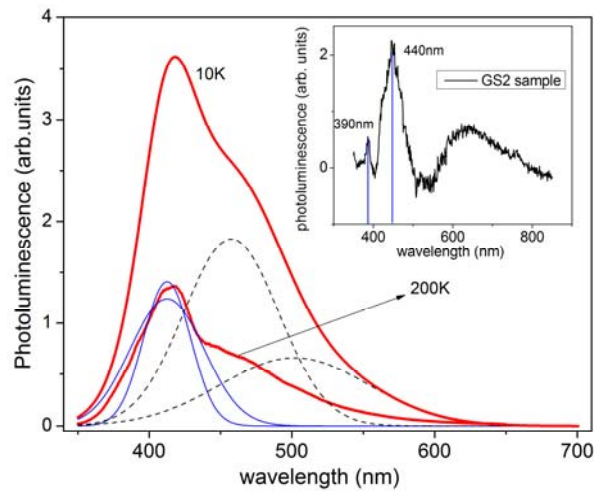


**Figure 2.** Photoluminescence for sample S Ce1000 at 10 K and 200 K, and deconvolution for PL at 10 K, where the blue bands are related  $Ce^{3+}$  emission. Broad band in dashed black are probably associated with defects in the  $SnO_2$  matrix. Excitation line: 325 nm of He–Cd laser. Inset: PL for heterostructured sample GSCe2. The blue vertical lines at 390 nm and 440 nm represent the probable  $Ce^{3+}$  transitions.

### 2.2. Electrical Characterization

Figure 3a shows conductance as a function of temperature for a GaAs/ $SnO_2$  heterostructured sample, GSCe3, measured in different conditions: in the dark and under the effect of irradiation with two different light sources: (1) InGaN LED (440–460 nm) and (2) a tungsten-halogen lamp plus a high pass filter, which cuts off wavelengths lower than 850 nm. Conductance as a function of temperature data is also shown in Figure 3b for a heterostructured sample deposited in the opposite order,  $SnO_2:1\%Ce^{3+}/GaAs$  (sample SGCe1), in the dark and under irradiation with the 4th harmonic of an Nd:YAG laser (266 nm).

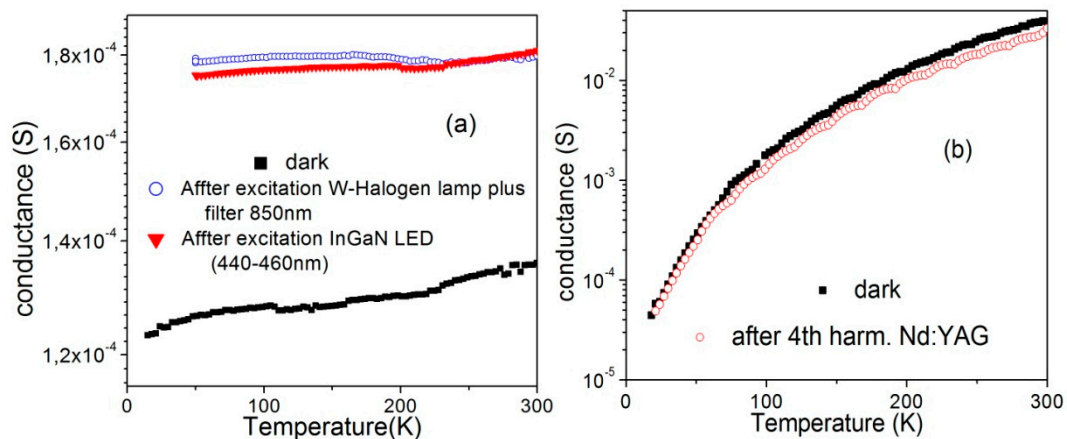


**Figure 3.** (a) Conductance as a function of temperature for heterostructured sample GSCe3, performed in the dark and under the effect of irradiation with different light sources: (1) InGaN LED (440–460 nm) (2) tungsten-halogen lamp plus an 850nm long pass filter. (b) conductance as a function of temperature for sample SGCe1 in the dark and after irradiation with the 4th harmonic of an Nd:YAG laser.

### 3. Discussion

#### 3.1. Optical Emission Properties

The heterostructure luminescence spectra shown in Figure 1 present a broad band as well as well-defined peaks. This broad band has its maximum at about 550 nm for the sample GSEu1, whereas the peak of the broad band is blue-shifted for the sample GSEu2, exhibiting a peak at about 470 nm. Moreover, the higher annealing temperature induces higher intensity for the whole spectra. The well-defined peaks are coincident with  $\text{Eu}^{3+}$  transitions:  ${}^5\text{D}_0 \rightarrow {}^7\text{F}_1$  (about 596 nm),  ${}^5\text{D}_0 \rightarrow {}^7\text{F}_2$  (about 618 nm), and  ${}^5\text{D}_0 \rightarrow {}^7\text{F}_4$  (about 704 nm). On the other hand, the emission spectrum of SEu500 film, directly deposited on the glass substrate without any bottom GaAs layer, presents a more intense broad band, but does not allow the identification of  $\text{Eu}^{3+}$  transitions. The PL emission of SEu1000 sample is also shown, evidencing the  $\text{Eu}^{3+}$ -dominant band changes, because the  ${}^5\text{D}_0 \rightarrow {}^7\text{F}_1$  transition is the most intense, unlike the PL for the heterostructure films deposited at low temperature, where the transition  ${}^5\text{D}_0 \rightarrow {}^7\text{F}_2$  turned out to be the most intense. It seems that the transition  ${}^5\text{D}_0 \rightarrow {}^7\text{F}_2$  intensity decreases for higher temperatures; it then may be postulated that it changes at some temperature for the  ${}^5\text{D}_0 \rightarrow {}^7\text{F}_1$  transition, which is the dominant for the  $\text{SnO}_2:2 \text{ at}\% \text{Eu}$  film, deposited on quartz substrate. The broad band peaks at 470 nm for the SEu500 film and at 445 nm for the SEu1000 film also exhibit a blue-shift with annealing temperature, for which the sample crystallite size is expected to increase. Discussion on the broad band is presented elsewhere [14]. It has been attributed either to electron transfer from oxygen vacancies to acceptor  $\text{Eu}^{3+}$  ions, or possibly to nanocrystalline defects, originating from the disorder in the material. However, the relevant point for this paper is that the heterostructure of  $\text{SnO}_2$  on top of the GaAs allows for the emission from the rare-earth ions, unlike films of  $\text{SnO}_2$  deposited directly on glass substrates, unless the thermal annealing temperature is very high.

Emission from  $\text{Ce}^{3+}$  in  $\text{SnO}_2$  could not be observed in films annealed at low temperature, which is similar to what happens in the case of Eu-doped  $\text{SnO}_2$  films. Although the sputtering sample presents a seemingly better interface and a better emission, only a small signal was recorded for the heterostructure, in which the bottom layer is GaAs-deposited by this technique. Thus, in order to make sure that  $\text{Ce}^{3+}$  has a recordable emission when incorporated in  $\text{SnO}_2$  films, a 1%Ce-doped  $\text{SnO}_2$  sample was deposited on quartz (SCe1000) and annealed at high temperature (1000 °C). Figure 2 shows the photoluminescence spectra for sample SCe1000 and the deconvolution of the PL spectra measured at 10 K. Although the emission at 200 K is evident, it has a much greater intensity at 10 K and is more adequate for the deconvolution procedure. In the inset of Figure 2,  $\text{Ce}^{3+}$  presents two emission bands (indicated by the blue vertical line), at 390 nm and 440 nm, which may correspond to transitions from 5d to 4f, reported in the literature in the range 350–420 nm ( ${}^2\text{F}_{5/2}$ ) and 380–470 nm ( ${}^2\text{F}_{7/2}$ ), respectively [21,22]. It seems that the observed emissions correspond to these transitions. The broad band for the SCe1000, revealed by the deconvolution process of the PL recorded at 10 K (dashed black curves), are probably related to the influence of the  $\text{SnO}_2$  matrix.

The obtained broad band from the deconvolution process, centered at 457 nm, may be attributed to deep level defects formed due to oxygen vacancies. Oxides are quite vulnerable to oxygen-related defects, and they can lead to additional negative charges when doped with different size ions—in this case with  $\text{Ce}^{3+}$ . These charges are compensated by the formation of oxygen vacancies. When a hole is trapped by an oxygen vacancy, it recombines with electrons from the conduction band, leading to the observed emission [23,24]. The broad band around 500 nm may be mainly associated with the presence of point defects, such as oxygen vacancies in  $\text{SnO}_2$  nanoparticles [25]. Similar broad bands are shown for the GaAs/ $\text{SnO}_2$  heterostructure, where the oxide is doped with  $\text{Eu}^{3+}$  (Figure 1). Considering the highly disordered condition of the  $\text{SnO}_2$  layer in the heterostructured sample, it is expected that this broad band will overcome the  $\text{Ce}^{3+}$  emission. A very faint Ce-related emission was obtained for the heterostructure, and the reproduction in the inset of Figure 2 became possible only due to the subtraction process. Again, two transitions from 5d to 4f are present. A more organized

condition of the GaAs bottom layer may lead to an oriented growth of the SnO<sub>2</sub> top layer and probably allows emission with better efficiency and thus allows signal separation.

### 3.2. Electrical Transport Properties

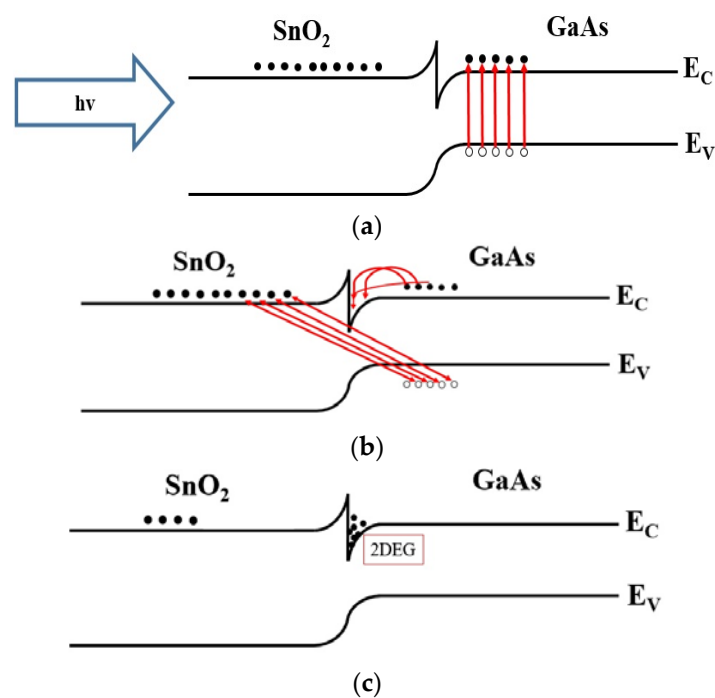
For the measurements with data shown in Figure 3a (sample GSCe3), the light source was focused on the sample for six minutes at low temperature before starting the temperature increase and the collecting of electrical current data. For the data obtained in the dark, it was observed that the sample has its conductance increased as the temperature is raised. However, when the sample is exposed to light excitation with an energy below the bandgap of SnO<sub>2</sub> and above the bandgap of GaAs, the heterostructure conductance increases significantly and remains constant as temperature increases. A possible explanation for this effect is the generation of electron-hole pairs in the GaAs, with the electrons drifting to the interface region (2DEG-like), where they remain confined. As these electrons remain trapped, there is a permanent change in electrical transport. On the other hand, the generated holes recombine with the electrons of the SnO<sub>2</sub> layer, located close to the interface, since there are electrons in excess in the SnO<sub>2</sub> layer, naturally n-type. Practically, no change is observed in electrical transport with temperature rise, because the trapped electrons at the interface are separated from scattering centers; thus, the electron mobility is not influenced by temperature, and the electron concentration at the interface (2DEG-like) remains constant. Therefore, the electrical conductivity is temperature-independent. The GaAs surface of the film deposited by sputtering is more suitable for this type of phenomenon, as inferred from the Atomic Force Microscopy (AFM) images (not shown) that display the smoother surface compared to the deposition by resistive evaporation. Another possibility for the observed conductivity behavior is that the wavelength is enough to ionize many intrabandgap states, and there is a very large density of scattering centers (shallow and deep donors and acceptors, extended defects, and grain boundaries) in the SnO<sub>2</sub> material that scattering by phonons is negligible. In this case, the other scattering phenomena would also have a compensated variation with temperature. Although possible, this possibility would include many processes; thus, the interface conduction phenomenon, as discussed, is more likely to occur. For the data in the inset of Figure 3b (sample SGCe1), a common behavior of semiconductors is observed in the dark with doping dominated by deep centers: its conductance decreases with cooling, which means that the decrease in carrier density overcompensates the expected increase in mobility. It is quite probable that the electric conduction only happens within the top GaAs layer. The irradiation with the laser does not change this behavior, although the Nd:YAG laser has a high intensity. The energy of the ultraviolet source is probably too high and is absorbed within a very short distance from the GaAs surface. Thus, the GaAs layer acts as a shield, preventing the light from reaching the SnO<sub>2</sub> layer. This behavior is similar to what was recorded for SnO<sub>2</sub>:Eu/GaAs, when the exact same light source was used [13].

Figure 4 shows a proposed model for the results of conductance as a function of the temperature presented in Figure 3. This model is sketched assuming the hypothesis of improved interface conduction. After light excitation, electron-hole generation in the GaAs layer takes place, assuming both light sources have an energy above the GaAs bandgap (Figure 4a). The electrons move towards the interface region, become confined at a 2DEG-like layer, and generate a permanent change in the conductance, because the electrons confined in the potential are well separated from the temperature-dependent scattering factors, such as ionized impurities and phonons. On the other hand, the holes recombine with electrons from the SnO<sub>2</sub> layer, which is an n-type material (Figure 4b). Then, when the temperature increases (Figure 4c), the conductance remains practically temperature-independent because the electrons become located at the 2DEG-like interface. Their concentration is practically independent of temperature, and they are not scattered by the temperature-dependent mechanisms, which indicates constant electronic mobility.

X-ray diffraction data for two heterostructure SnO<sub>2</sub>/GaAs:Ce<sup>3+</sup> samples, grown in both deposition orders (not shown) present the diffuse profile typical of a nano-crystallized domain, which tends to support the hypothesis of a high orientation disorder within both the GaAs and SnO<sub>2</sub> layers,

as expected for these sorts of substrates and deposition techniques. The few observed peaks correspond to the planes of tin dioxide with the rutile structure and planes of zinc-blended GaAs. It is important to recall the low thermal annealing temperature of the SnO<sub>2</sub> layer in the case of SnO<sub>2</sub> on top of GaAs, because 150 °C is quite low for crystallizing SnO<sub>2</sub>; however, if a higher temperature is used, it could degrade the GaAs layer. Thus, it is easily concluded that there is a great structural disorder in this sample, and one should expect very small crystallites.

It is important to mention that indications of the effect of confinement in a 2DEG-like potential has been found before [13]. Although the deposition procedures of these layers do not suggest that a 2DEG formation is possible for the samples, the obtained effect on the conductance indicates that some sort of interfacial conduction improvement is being generated. Thus, coupling this conductivity effect with the emission obtained from rare-earth doping in the top SnO<sub>2</sub> layer, leads to very interesting features that have potential for application in optoelectronic devices such as light-modulated high-mobility field effect transistors.



**Figure 4.** Model for the behavior of the temperature-dependent conductance data. Two-dimensional electron gas (2DEG); (a) Sample is illuminated with above GaAs bandgap light on the SnO<sub>2</sub> side (top layer). (b) excited electrons from the GaAs side migrate to the interface region and GaAs holes recombine with SnO<sub>2</sub> electrons. (c) decrease of the electron population in the SnO<sub>2</sub> layer and interfacial region (2DEG-like) becomes populated; E<sub>C</sub>: conduction band, E<sub>V</sub>: valence band.

## 4. Materials and Methods

### 4.1. Synthesis of Heterostructure

The resulting suspension, used for deposition of thin films, was produced by the sol–gel process from solutions of SnCl<sub>4</sub>·5H<sub>2</sub>O and Ce(NO<sub>3</sub>)<sub>3</sub>·6H<sub>2</sub>O. SnO<sub>2</sub> films were deposited by the dip-coating technique on borosilicate glass substrates with a withdrawal rate of 10 cm/min. Layers were deposited at room temperature, gelling in air for 20 min and heated at 400 °C for 10 min in a furnace at room pressure. When the total of the desired layers was reached, samples were submitted to thermal annealing, which generally is at 500 °C for 1 h in the same furnace. Resulting thickness of films obtained by this procedure is about 300 nm [13]. The intermediate thermal treatment between layers was absent in the case where the SnO<sub>2</sub> film was deposited on top of GaAs. In this case, the final annealing was

for 150 °C for 1 h, a procedure that does not damage the GaAs bottom layer. The deposition of the Eu<sup>3+</sup>-doped SnO<sub>2</sub> thin film layer has been described in detail elsewhere [7]. The deposition also took place in an air atmosphere (room temperature), and samples, after each layer, are dried in air for 20 min and treated at 200 °C for 10 min in the same oven used for GaAs annealing. This procedure was repeated 10 times. The final annealing was at 200 °C for 1 h (sample GSEu1) or 400 °C for 20 min (sample GSEu2) for different samples. In the case of the SnO<sub>2</sub> film sample without GaAs, deposited directly on the glass substrate, the final annealing was at 500 °C for 1 h (sample SEu500); in the case of the SnO<sub>2</sub>:2%Eu film deposited directly on a quartz substrate, the final annealing was at 1000 °C for 1 h (sample SEu1000).

GaAs films and In electrodes were evaporated through the resistive evaporation technique. Metallic In deposition was carried out to make electric contacts to the films in order to accomplish electrical measurements. These materials were deposited with  $7 \times 10^{-6}$  torr of pressure in an Edwards Auto 500 evaporation system (Edwards, Crawley, United Kingdom) using a tungsten crucible. Resistively evaporated GaAs were submitted to thermal annealing at 150 °C for 1 h. In electrodes were submitted to thermal annealing at 150 °C for 30 min. In the case of samples doped with Eu<sup>3+</sup>, all GaAs layers were deposited by this technique. In the case of samples doped with Ce<sup>3+</sup>, some GaAs samples were deposited by the sputtering technique. In this case, the deposition was carried out in a purpose-built system [26] using 30 W of radio frequency (RF) power, an Ar-flux of 30 standard cubic centimeters per minute (sccm), and a pressure of  $4.5 \times 10^{-2}$  torr for 60 min. The average substrate temperature during deposition was about 20 °C.

Samples where the SnO<sub>2</sub> layer is doped with Ce<sup>3+</sup> are deposited as follows: (1) sample S Ce1000 (SnO<sub>2</sub>:1%Ce<sup>3+</sup>): a sol-gel-dip-coating-deposited SnO<sub>2</sub> layer doped with 1%Ce<sup>3+</sup> on a quartz substrate with 15 layers (a thickness of about 300 nm), thermally annealed at 1000 °C for 1 h; (2) SG Ce1 (SnO<sub>2</sub>:1%Ce<sup>3+</sup>/GaAs): bottom: 10 layers of 1%Ce<sup>3+</sup>-doped SnO<sub>2</sub> deposited on a soda-lime glass substrate and annealed at 500 °C for 1 h; top: resistive evaporated GaAs, annealed at 150 °C for 30 min; (3) G S Ce2 (GaAs/SnO<sub>2</sub>:1%Ce<sup>3+</sup>): bottom: GaAs deposited by sputtering on a silica glass substrate; top: 30 layers of 1%Ce<sup>3+</sup>-doped SnO<sub>2</sub> annealed at 150 °C for 30 min; (4) G S Ce3 (GaAs/SnO<sub>2</sub>:1%Ce<sup>3+</sup>): bottom: GaAs deposited by sputtering on a Si (100) substrate; top: 10 layers of 1%Ce<sup>3+</sup>-doped SnO<sub>2</sub>, annealed at 150 °C for 30 min. Labels S (SnO<sub>2</sub>) and G (GaAs) indicate the deposition order.

#### 4.2. Electrical and Optical Characterization

Conductance as a function of temperature was carried out under vacuum conditions, in a helium closed circuit cryostat (Janis Research, Woburn, MA, USA), coupled with a Lake Shore temperature controller. The electrical data were collected using a Keithley electrometer, model 617 (Keithley Instruments Inc., Cleveland, OH, USA). The following light sources are used to provide excitation to the electrical transport properties: (1) the 4th harmonic (266 nm) of a Nd:YAG pulsed laser, with 4.8 mJ of energy and 10 Hz of pulse frequency; (2) an InGaN LED (440–460 nm) and 15 W of power; (3) a tungsten-halogen lamp (150 W) plus a long-pass filter, which cuts off wavelengths lower than 850 nm. For the PL measurements of the GaAs/SnO<sub>2</sub>:Ce<sup>3+</sup> samples, samples were excited with the 325 nm line of a He–Cd laser, and the signal was detected by a GaAs photomultiplier detector cooled with liquid nitrogen. A single configuration monochromator was used for selecting the emitted signal. For the PL measurements of the GaAs/SnO<sub>2</sub>:Eu<sup>3+</sup> samples, samples were excited with a modulated 350 nm line of a Krypton (Kr<sup>+</sup>) laser, and the signal was detected by an R955 PMT (Hamamatsu, Shimokanzo, Japan) and an SR530 Lock-in Amplifier (Stanford Research, Palo Alto, CA, USA).

### 5. Conclusions

Doping SnO<sub>2</sub> thin films with Eu<sup>3+</sup> leads to interesting luminescent emissions from rare-earth ions when the doped tin dioxide film is grown on the top of the GaAs layer, unlike SnO<sub>2</sub> deposition grown directly on a glass substrate. The Eu emission comes along a broad band that is present in all films and that blue-shifts as the thermal annealing temperature increases. Luminescence from the Ce<sup>3+</sup> ions in

the heterostructure can be obtained, as the emissions from the rare-earth ions can be separated from the matrix emission. The ions are very close and overlap.

The temperature variation has little influence on the conductance, which is practically constant. This unusual behavior was associated with GaAs/SnO<sub>2</sub> interfacial conduction, which might be associated with the presence of two-dimensional electron gas small channels (2DEG-like). The deposition order of layers as well as the GaAs deposition method is fundamental for providing excitation of the interfacial channel. When GaAs is at the bottom, the interfacial channel can be excited by light with energy intermediate between the SnO<sub>2</sub> and the GaAs bandgaps. Energies above the SnO<sub>2</sub> bandgap only excite the oxide top layer. When the GaAs is at the top, it acts as a radiation shield.

The luminescence from trivalent rare-earth (RE<sup>3+</sup>)-doped oxides in the form of thin films provides accessibility to construction and the operation of luminescent and electroluminescent devices. In addition, the possibility of temperature-independent conduction of the interface opens new possibilities for application in optoelectronic devices, combining the RE<sup>3+</sup> emission with high electron mobility, making the operation of electroluminescent devices easier and faster.

Part of this work has been presented at the international conference on Atomically Controlled Surfaces Interfaces and Nanostructures ACSIN 2016 held in Frascati, Rome, Italy, on 9–15 October 2016 [27].

**Acknowledgments:** The authors would like to thank Andre L. J. Pereira and José H. D. da Silva for the preparation of the GaAs films by sputtering, Américo Tabata and Maximo S. Li for help with photoluminescence measurements, Brazilian agencies CAPES and CNPq (grant 471359/2013-0), and grants 2006/00480-9 and 2016/12216-6 from the São Paulo Research Foundation (FAPESP).

**Author Contributions:** Diego H. O. Machado performed the experiments with Ce<sup>3+</sup>-doped SnO<sub>2</sub> samples and Cristina F. Bueno performed the experiments with Eu<sup>3+</sup>-doped SnO<sub>2</sub> samples; Luis V. A. Scalvi supervised the experiments and wrote the paper.

**Conflicts of Interest:** The authors declare no conflict of interest.

## References

1. Ray, S.C.; Karanjai, M.K.; Dasgupta, D. Tin dioxide based transparent semiconducting films deposited by the dip-coating technique. *Surf. Coat. Technol.* **1998**, *102*, 73–80. [[CrossRef](#)]
2. Ishii, M.; Komuro, S.; Morikawa, T. Study on atomic coordination around Er doped into anatase- and rutile-TiO<sub>2</sub>: Er-O clustering dependent on the host crystal phase. *J. Appl. Phys.* **2003**, *94*, 3823–3827. [[CrossRef](#)]
3. Peng, H.; Song, H.; Chen, B.; Wang, J.; Lu, S.; Kong, X.; Zhang, J. Temperature dependence of luminescent spectra and dynamics in nanocrystalline Y<sub>2</sub>O<sub>3</sub>: Eu<sup>3+</sup>. *J. Chem. Phys.* **2003**, *118*, 3277–3282. [[CrossRef](#)]
4. Yang, X.; Jurkovic, M.J.; Heroux, J.B.; Wang, W.I. Molecular beam epitaxial growth of InGaAsN: Sb/GaAs quantum wells for long-wavelength semiconductor lasers. *Appl. Phys. Lett.* **1999**, *75*, 178–180. [[CrossRef](#)]
5. Sze, S.M. *Physics of Semiconductor Devices*; John Wiley & Sons: New York, NY, USA, 1985.
6. Yu, L.; Song, H.; Lu, S.; Liu, Z.; Yang, L.; Wang, T.; Kong, X. Thermal quenching characteristics in LaPO<sub>4</sub>:Eu nanoparticles and nanowires. *Mater. Res. Bull.* **2004**, *39*, 2083–2088. [[CrossRef](#)]
7. Morais, E.A.; Scalvi, L.V.A.; Tabata, A.; De Oliveira, J.B.B.; Ribeiro, S.J.L. Photoluminescence of Eu<sup>3+</sup> ion in SnO<sub>2</sub> obtained by sol-gel. *J. Mater. Sci.* **2008**, *43*, 345–349. [[CrossRef](#)]
8. Dorenbos, P. 5d-level energies of Ce<sup>3+</sup> and the crystalline environment. III. Oxides containing ionic complexes. *Phys. Rev. B Condens. Matter Mater. Phys.* **2001**, *64*, 125117. [[CrossRef](#)]
9. Annapurna, K.; Dwivedi, R.N.; Kundu, P.; Buddhudu, S. Blue Emission spectrum of Ce<sup>3+</sup>: ZnO-B<sub>2</sub>O<sub>3</sub>-SiO<sub>2</sub> optical glass. *Mater. Lett.* **2004**, *58*, 787–789. [[CrossRef](#)]
10. Mao, Z.; Zhu, Y.; Wang, Y.; Gan, L. Ca<sub>2</sub>SiO<sub>4</sub>: Ln (Ln<sup>5</sup> Ce<sup>3+</sup>, Eu<sup>2+</sup>, Sm<sup>3+</sup>) tricolor emission phosphors and their application for near-UV white light-emitting diode. *J. Mater. Sci.* **2014**, *49*, 4439–4444. [[CrossRef](#)]
11. Zhang, H.; Fu, X.; Niu, S.; Sun, G.; Xin, Q. Luminescence properties of Li<sup>+</sup> doped nanosized SnO<sub>2</sub>:Eu. *J. Lumin.* **2005**, *115*, 7–12. [[CrossRef](#)]
12. Gu, F.; Wang, S.F.; Lu, M.K.; Qi, Y.X.; Zhou, G.J.; Xu, D.; Yuan, D.R. Luminescent characteristics of Eu<sup>3+</sup> in SnO<sub>2</sub> nanoparticles. *Opt. Mater.* **2004**, *25*, 59–64. [[CrossRef](#)]

13. Pineiz, T.F.; Morais, E.A.; Scalvi, L.V.A.; Bueno, C.F. Interface formation of nanostructured heterojunction SnO<sub>2</sub>: Eu/GaAs and electronic transport properties. *Appl. Surf. Sci.* **2013**, *267*, 200–205. [[CrossRef](#)]
14. Bueno, C.F.; Scalvi, L.V.A.; Li, M.S.; Saeki, M.J. Luminescence of Eu<sup>3+</sup> in the thin film heterojunction GaAs/SnO<sub>2</sub>. *Opt. Mater. Express* **2015**, *5*, 59–72. [[CrossRef](#)]
15. Tan, S.T.; Zhao, J.; Iwan, S.; Su, X.W.; Tang, X.; Ye, J.; Bosman, M.; Tang, L.J.; Lo, G.-Q.; Teo, K.L. n-ZnO/n-GaAs heterostructured white light-emitting diode: Nanoscale analysis and electroluminescence studies. *IEEE Trans. Electron. Devices* **2010**, *57*, 129–133. [[CrossRef](#)]
16. Cuculescu, E.; Evtodiev, I.; Caraman, M. Non-equilibrium charge carriers generation—Recombination mechanisms at the interface of the SnO<sub>2</sub>/GaSe heterojunction. *Thin Solid Films* **2009**, *517*, 2515–2518. [[CrossRef](#)]
17. Vataavu, S.; Zhao, H.; Caraman, I.; Gasin, P.; Ferekides, C. Photoluminescence studies of CdTe/SnO<sub>2</sub> and CdTe/CdS heterojunctions: The influence of oxygen and the CdCl<sub>2</sub> heat treatment. *Thin Solid Films* **2011**, *519*, 7176–7179. [[CrossRef](#)]
18. Maciel, J.L.B., Jr.; Floriano, E.A.; Scalvi, L.V.A.; Ravaro, L.P. Growth of Al<sub>2</sub>O<sub>3</sub> thin film by oxidation of resistively evaporated Al on top of SnO<sub>2</sub>, and electrical properties of the heterojunction SnO<sub>2</sub>/Al<sub>2</sub>O<sub>3</sub>. *J. Mater. Sci.* **2011**, *46*, 6627–6632. [[CrossRef](#)]
19. Wang, E.Y.; Legge, R.N. General properties of SnO<sub>2</sub>-GaAs and SnO<sub>2</sub>-Ge heterojunction photovoltaic cells. *IEEE Trans. Electron. Devices* **1978**, *25*, 800–803. [[CrossRef](#)]
20. Bark, C.W.; Sharma, P.; Wang, Y.; Beak, S.H.; Lee, S.; Ryu, S. Switchable Induced Polarization in LaAlO<sub>3</sub>/SrTiO<sub>3</sub> Heterostructures. *Nano Lett.* **2012**, *12*, 1765–1771. [[CrossRef](#)]
21. Bian, L.; Du, F.; Yang, S.; Ren, Q.; Liu, Q.L. Crystal structure and near-ultraviolet photoluminescence properties of Ba<sub>9</sub>Sc<sub>2</sub>Si<sub>6</sub>O<sub>24</sub>: Ce<sup>3+</sup>, Na. *J. Lumin.* **2013**, *137*, 168–172. [[CrossRef](#)]
22. Fang, Z.; Cao, R.; Zhang, F.; Ma, Z.; Dong, G.; Qiu, J. Efficient spectral conversion from visible to near-infrared in transparent glass ceramics containing Ce<sup>3+</sup>-Yb<sup>3+</sup> codoped Y<sub>3</sub>Al<sub>5</sub>O<sub>12</sub> nanocrystals. *J. Mater. Chem. C* **2014**, *2*, 2204–2211. [[CrossRef](#)]
23. Inpasalini, M.S.; Singh, A.; Mukherjee, S. Luminescence and magnetism studies of strongly quantum confined SnO<sub>2</sub> dots. *J. Mater. Sci.: Mater. Electron.* **2016**, *27*, 4392–4398. [[CrossRef](#)]
24. Ko, S.L.; Park, S.; Kim, C.-W.; Lee, D.; Choi, M.S.; Lee, C.; Jin, C. Shape-selective synthesis and photoluminescence of SnO<sub>2</sub> nanostructures under different catalyst conditions. *Appl. Phys. A* **2015**, *121*, 715–721. [[CrossRef](#)]
25. Sánchez Zeferino, R.; Pal, U.; Meléndrez, R.; Barboza Flores, M.; Barboza, M. PL and TL behaviors of Ag-doped SnO<sub>2</sub> nanoparticles: Effects of thermal annealing and Ag concentration. *Adv. Nano Res.* **2013**, *1*, 193–202. [[CrossRef](#)]
26. Azevedo, G.D.; Silva, J.H.D.; Avendano, E. Effect of hydrogenation on the optical and structural properties of GaAs thin films prepared by rf-magnetron sputtering. *Nucl. Instrum. Methods Phys. Res. Sect. B-Beam Interact. Mater. Atoms* **2005**, *238*, 329–333. [[CrossRef](#)]
27. Acun, A.; Akaishi, A.; Angot, T.; Araidai, M.; Aristov, V.; Aruga, T.; Avdeev, M.; Banas, K.; Banas, A.; Banhart, F.; et al. *Atomically Controlled Surfaces Interfaces and Nanostructures*; Bianconi, A., Marcelli, A., Eds.; Superstripes Press: Rome, Italy, 2016.

